A cost-effective beam forming structure for GNSS multipath mitigation and its assessment

Qiongqiong Jia [1,2], Li-Ta Hsu [1], Bing Xu [1] and Renbiao Wu [2]

[1] *(Interdisciplinary Division of Aeronautical and Aviation Engineering, The Hong Kong) Polytechnic University*

[2] *(Tianjin Key Lab for Advanced Signal Processing, Civil Aviation University of China)*

(E-mail: lt.hsu@polyu.edu.hk**)**

Array antenna beam forming is in high potential to improve performance of Global Navigation Satellite System (GNSS) in urban areas. However, the widespread application of array antenna for GNSS multipath mitigation is restricted by many factors, such as the complexity of the system, the computation load and the conflicts among the required performance, the cost budget and the limited room for the antenna placement. The scope of this work are triplicate. 1) The pre-correlation beam forming structure is firstly suggested for multipath mitigation to decrease the system complexity. 2) With the pre-correlation structure, the equivalence of adaptive beam forming to the quiescent one is revealed. Therefore, the computation load for beam forming is greatly decreased. 3) A theoretical model is established to link the profits of beam forming with GNSS performance improvement in terms of pseudorange quality. The model can be used by the industry to balance the aforementioned restrictions. Numerical results with different array settings are given, and a 2 by 2 rectangle array with 0.4λ element spacing is suggested for a cost-effective choice in GNSS positioning applications in urban canyon areas.

KEYWORDS

GNSS; Array Antenna; Beam Forming; Multipath; Urban Canyon

1. INTRODUCTION. Global Navigation Satellite System (GNSS) is widely used in military and civilian areas for Position, Velocity and Time (PVT). Due to the weak power when reaching the earth surface, GNSS signal is very vulnerable to various intentional and unintentional interference (Amin et al. 2016; Sahmoudi and Amin 2009; Fohlmeister et al. 2017; Sgammini et al. 2019; Appel et al. 2019; Fernandez-Prades et al. 2016; García-Molina and Fernández-Rubio 2019). Among which, the ubiquity multipath is notably difficult to address, especially for mobile devices operating in urban areas (Hsu et al. 2015; Sun et al. 2020; Xie and Petovello 2015). Multipath reflected by the high rising buildings greatly degrades the positioning performance. Multipath induced pseudorange error is up to hundreds of meters, hence significant research have been devoted to multipath mitigation (Seco-Granados et al. 2005; Jia et al. 2017).

Advanced antenna designs, such as choke ring (Tranquilla et al. 1994) and dual-polarized (Sgammini et al. 2019; Xie et al. 2017) antenna are well-known techniques to reduce multipath effect. Choke ring antenna rejects low elevation receptions, which is effective to ground reflection. However, it is ineffective in urban areas, where multipath reflected from buildings share similar elevation angle to the Line Of Sight (LOS) signal (Hsu 2018). Dual-polarized antenna utilizes the signal axial variation during reflection, which does not work for multi-bounce reflection (Fohlmeister et al. 2017; Markus et al. 2016).

By excluding or down weighting the multipath contaminated measurement, multipath effect on the PVT solution can be decreased (Realini and Reguzzoni 2013; Groves and Jiang 2013; Sun et al. 2020; Sun et al. 2019). However, it's difficult to accurately classify the measurement such as pseudorange or signal strength, for the false measurement from multipath contaminated data sometimes is similar to the correct one from other clean data (Hsu 2017; Aram et al. 2007; Alnaqbi and El-Rabbany 2010). Therefore, signal processing methods are much preferred to deal with contaminated data from its source. Signal processing methods based on single antenna and antenna array are listed below.

1.1. Techniques for single antenna. For conventional receivers with a single antenna, advanced correlator-based methods, such as narrow correlator, strobe correlator, High Resolution Correlator (HRC) (R.D.J. van Nee 1992a; Gary and Michael 1999; Tranquilla et al. 1994; Wang and Huang 2019), etc. were proposed to suppress the multipath. The correlator-based methods only need minor changes to the off-the-shelf receiver, hence they have been widely implemented.

To further improve the multipath mitigation performance, multipath parameter estimation based methods, e.g. Multipath Mitigation Delay Lock Loop (MEDLL) (Bryan and Patrick 1995; R.D.J. van Nee 1992b; Wang and Huang 2019), Multipath Elimination Technique (MET) (Bryan and Patrick 1994) and Weighted RELAXation (WRELAX) (Jia et al. 2017), etc., were proposed. Although performance is improved, they are challenged by the computation load and require major change of the receiver structure (Tamazin et al. 2016). Besides, all of these temporal domain methods are ineffective to short delay multipath.

Aside from the temporal domain methods, the frequency domain methods based on the Doppler difference was also reported (Xie and Petovello 2015; Sokhandan et al. 2014; Alnaqbi and El-Rabbany 2010; Aram et al. 2007). However, the minor Doppler difference requires much longer coherent integration period, which is restricted by the navigation data bit transition and the oscillator instability (Xie and Petovello 2015).

1.2. Techniques for array antenna. By exploiting the spatial diversity, array antenna is able to improve the robustness of GNSS receiver. The array antenna can be used either un-structurally without using the array manifold (García-Molina and Fernández-Rubio 2019; Garca-Molina et al. 2018) or structurally using the array manifold (Broumandan et al. 2016). The un-structurally use of array antenna in the GNSS literature models the problem as a Multiple-Input Multiple-Output (MIMO) unambiguous position estimation problem, which has the superiority of robust to array error, whereas, it faces much more computational load in solving the multi-dimensional non-linear cost function (García-Molina and Fernández-Rubio 2019; J. A. Garcia-Molina and J. A. Fernandez-Rubio 2018). The structurally use of array antenna such as spatial beam forming is more popular. By weighting the reception from different array elements (Figure 1(a)), spatial adaptive beam forming is able to point main beam gain in the Direction Of Arrival (DOA) of the desired satellite signal and/or null in the interference direction. It has the ability to separate signals overlapped in frequency and temporal domains due to the usage of spatial DOA information. The superiority of array antenna beam forming attracts comprehensive study for mitigation of high power interference such as jamming (Fernandez-Prades et al. 2016; Li et al. 2014), continuous wave (CW) interference (Min Li et al. 2011) and low power interference such as spoofing (Cuntz et al. 2016) and multipath (Daneshmand et al. 2013). Although focus here is multipath mitigation, high power interference mitigation is briefly reviewed first to help address the special issues for multipath mitigation.

Power Inversion (PI) can form beam null in the high power interference direction. The adaptive beam forming weight of PI is the inversion of the spatial correlation matrix, which is calculated

by the pre-correlation data (Wu et al. 2018). Hence PI is implemented in a pre-correlation structure, as shown in Figure 1(b). To further enhance the satellite signal quality while nulling high power interference, beam gain can be formed in each satellite direction (Jia et al. 2018; Daneshmand et al. 2013). The beam gain forming weight can be obtained by using the DOA from the satellite ephemeris and the coarse receiver position, hence it can be implemented as the pre-correlation structure (Figure 1(c)) (Daneshmand et al. 2013; Broumandan et al. 2016). In the pre-correlation structure, beam forming is implemented for each satellite signal, and then each output is sent to the corresponding tracking channel. Therefore, the pre-correlation beam forming structure is compatible to the off-the-shelf receiver with only minor change of the data source for the tracking channel.

Unlike the high power jamming and interference, multipath is the time-delayed replica of the LOS signal. Difficulties and countermeasures of beam forming for multipath mitigation are listed below.

(1) Multipath is submerged into noise before correlation due to its low power characteristic. Beam null forming weight is obtained after correlation in many approaches such as multipath DOA estimation (Wu et al. 2018), multipath eigenvector estimation (Appel et al. 2019; Daneshmand et al. 2013), robust beam forming (Vicario et al. 2010) and hybrid beam forming (Fernandez-Prades et al. 2016; Seco-Granados et al. 2005). Hence, a post-correlation structure is required, as shown in Figure 1(d).

(2) The high correlation between the LOS signal and the multipath component will result in signal cancellation and correlation matrix rank deficiency, leading to severe performance degradation or completely fail of the conventional adaptive beam forming methods such as Minimum Power Distortionless Response (MPDR) and Linear Constraint Minimum Power (LCMP). Spatial smoothing (Appel et al. 2019; Broumandan et al. 2016) and moving antenna (S. Daneshmand et al. 2013) were proposed to deal with this problem.
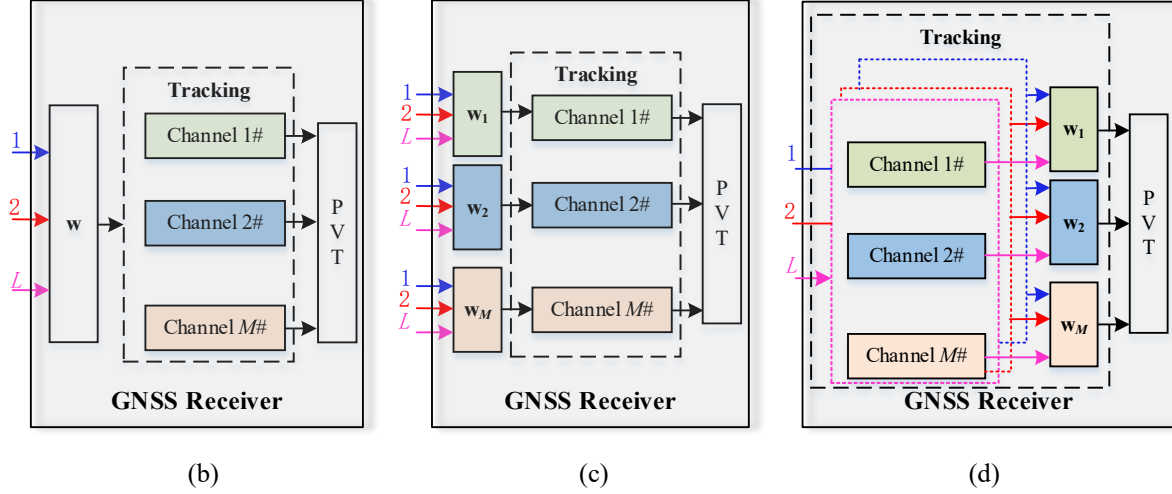

(a)
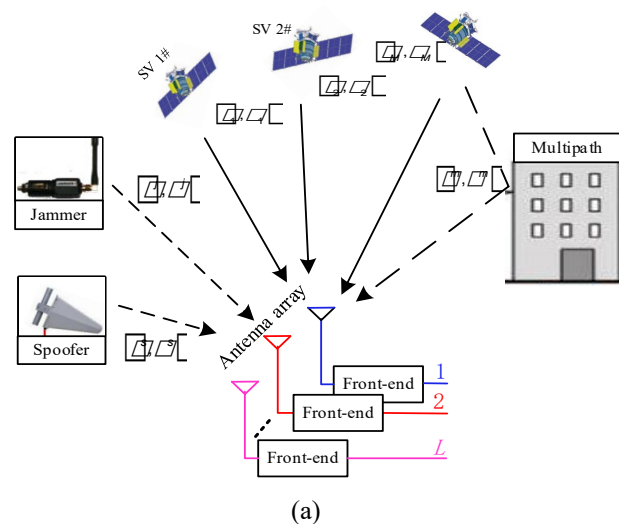
Figure 1 - Antenna array beam forming in GNSS receiver: (a) array antenna reception, (b) pre-correlation structure for single beam forming, (c) pre-correlation structure for multiple beam forming and (d) post-correlation structure.

1.3. Gaps between Literature and industry. Despite of the existing literatures on array antenna beam forming based multipath mitigation, there are still certain gaps restricting its application, especially for low-cost devices such as mobile devices.

1) The post-correlation structure for multipath mitigation in Figure 1(d) requires a major change of the off-the-shelf receiver structure. A number of extra tracking channels are required since signals from each array element need to be processed.

2) Estimation quality of beam null forming weight is restricted by array aperture. The aperture is proportional to the array antenna element number and the element spacing, which is limited by the cost budget and available room for antenna.

3) Countermeasures for signal cancellation and rank deficiency problem is faced with array aperture loss (spatial smoothing) or requirement of rigorous system control (moving array).

4) The state-of-the-art performance analysis is given by providing some experiment scenarios with specific parameters (García-Molina and Fernández-Rubio 2019; Vagle et al. 2016a; Vagle et al. 2016b). Whereas, the beam forming performance is greatly related to the array setting and the source signal parameters. Besides, the performance metrics is seldom linked to GNSS measurement. Therefore, there is a shortage of comprehensive and straight-forward performance assessment to convince the industry community for the wide application of array antenna.

1.4. Contributions of This Paper. To close the previously mentioned gaps, this is the first paper that provides the following contributions. 1) The pre-correlation structure that is compatible to the off-the-shelf receiver, is suggested for multipath mitigation in low-cost urban positioning applications with reduced system complexity. 2) Based on the pre-correlation structure, this paper reveals the fact that the data dependent adaptive beam forming for multipath mitigation is equivalent to the corresponding data independent quiescent beam forming (van Veen 1990). Hence not only the signal cancellation and covariance matrix rank deficiency issues are avoided, but also the computation load for beam forming is greatly decreased. 3) Analytical models are established to evaluate the array beam forming introduced profits, where pseudorange quality is used as the performance metric. The established models can serve as an evaluation tool for industry to balance the required performance, available room for antenna placement and cost budget.

A descriptive comparison between our solution and the representative works in the literature is provided in Table I. A review of the multipath mitigation methods shows the necessity of introducing array antenna. The rapid development of the GNSS antenna and electronics industry also provides chances for low cost and small bulk size GNSS antenna (Caizzone et al. 2016; Volakis et al. 2016). With this premise, and with the suggested structure and the evaluation model built in this paper, improved positioning performance can be expected in mobile devices.

The paper is organized as follows. Firstly, array beam forming basic is given section 2. Then the quiescent beam forming structure with low system complexity and computation load is proposed for urban positioning application in section 3. Thirdly, the beam forming performance assessment models are derived in an analytical way in section 4. In section 5, numerical results of the assessment models and Monte Carlo simulations are given. Finally, a summary and a suggestion to the antenna array setting for low-cost urban applications are given.

TABLE I

TYPICAL MULTIPATH MITIGATION METHODS

		Typical technique	Receiver structure change	Cons.
Antenna design		Choke-ring	No	♦ No elimination of high-elevation multipath
		Dual-polarized antenna	No	♦ Not effective for multi-bounce multipath
Measurement processing		Exclusion or down weighting, etc.	No	♦ Measurement classify accuracy is limited
Signal proces-sing	Correlator design	Narrow correlator, Strobe correlator, HRC etc.	Minor revision in DLL	♦ Not applicable to short delay multipath
	Parameter estimation	MEDLL, MET, WRELAX, etc.	Major revision in DLL	♦ High computation load ♦ Limited performance to short delay multipath
	Frequency discriminat-ion	Improved correlator peak selection	Tracking loop should be aided by navigation data	♦ Extend the coherent integration period ♦ Performance limited by the oscillator stability
	Array antenna	Post-correlation beam forming	Times of tracking loop are required	♦ More resources and high computation load ♦ DOA estimation is required for beamforming
		Pre-correlation beam forming	No	♦ Ray tracing and 3D city model are required for LCMP

DLL: Delay Lock Loop

2. BASIC OF BEAM FORMING. GNSS performance in urban area can be improved by increasing the C/N_0 to reduce the variance of the measurement and by decreasing the multipath signal component to eliminate the multipath introduced bias. Beam forming has the advantage of steering main beam gain to increase the C/N_0, meanwhile, multipath falls into the low side lobe or the beam null will be attenuated. Therefore, antenna array beam forming has a great potential to improve the GNSS performance in urban canyon area. The antenna array received data model is given firstly, then two popular beam forming algorithms are given in this section.

2.1. Data model. The signal in (3) received by an array antenna is given by

$$\mathbf{x}(t) = \sum_{p=0}^{P} \iota_p s_p(t) \mathbf{a}(\theta_p, \varphi_p) + \mathbf{x}_n(t) \tag{1}$$

where $\mathbf{x}_n(t)$ stands for the noise vector, which is modeled as a zero mean Gaussian process with variance σ_n^2. The satellite signals and multipath are assumed to be independent to the noise. The signal waveform is $s_p(t) = \iota_p D(t - \tau_p) c(t - \tau_p) e^{j\phi_p t}$, with ι, τ and ϕ representing amplitude, code phase and carrier phase residual, respectively. The subscripts $p = 1, ..., P$ denotes the multipath index and $p = 0$ stands for the LOS signal. $D(t)$ denotes the navigation data, and $c(t)$ is the C/A code. The array steering vector $\mathbf{a}(\theta, \varphi)$ is expressed as (Wu et al. 2018)

$$\mathbf{a}(\theta, \varphi) = \begin{bmatrix} e^{-j\mathbf{u}^T\mathbf{p}_1} & e^{-j\mathbf{u}^T\mathbf{p}_2} & ... & e^{-j\mathbf{u}^T\mathbf{p}_L} \end{bmatrix}^T \tag{2}$$

where (θ, φ) are the azimuth and elevation, respectively, $\mathbf{u} = 2\pi d/\lambda \begin{bmatrix} \sin\theta\cos\varphi & \sin\theta\sin\varphi & \cos\theta \end{bmatrix}^T$ is the wave vector with d denoting the element space. The 3D position of the l th array element is $\mathbf{p}_l = \begin{bmatrix} x_l, & y_l, & z_l \end{bmatrix}^T$, where $l = 1, 2, ..., L$ and L is the array element number.

The high rising building-reflected signal in urban areas shares nearly the same elevation with the LOS signal (Hsu 2018), which means $\varphi_p \approx \varphi_0, p = 1, ..., P$, then the steer vector in (2) can be simplified to $\mathbf{a}_p = \mathbf{a}(\theta_p, \varphi_0)$. Without loss of generality, the case of one reflected multipath is discussed in this paper firstly, hence (1) can be simplified to

$$\mathbf{x}(t) = \mathbf{x}_s(t) + \mathbf{x}_m(t) + \mathbf{x}_n(t) \tag{3}$$

where $\mathbf{x}_s(t)$ and $\mathbf{x}_m(t)$ stand for the LOS and multipath components respectively. The core of beam forming is to find an appropriate weight for forming expected beams. Two conventional beam forming methods are given below.

2.2. MPDR. The objective function of the MPDR beam forming can be formulated as (Jia et al. 2018)

$$\begin{cases} \min \ \mathbf{w}_{MPDR}^H \mathbf{R} \mathbf{w}_{MPDR} \\ \text{s.t.} \ \mathbf{w}_{MPDR}^H \mathbf{a}_0 = 1 \end{cases} \tag{4}$$

where $\mathbf{R} = \mathrm{E}\begin{bmatrix} \mathbf{x}\mathbf{x}^H \end{bmatrix}$ is the covariance matrix of $\mathbf{x}(t)$. The first row in (4) is to minimize the power of the received data, while the second row is to constrain the expected LOS without distortion. Hence the MPDR beam forming has the capability of pointing main beam in LOS direction while minimizing multipath reception from all other directions. The solution to (4) is

$$\mathbf{w}_{MPDR} = \left(\mathbf{a}_0^H \mathbf{R}^{-1} \mathbf{a}_0 \right)^{-1} \mathbf{R}^{-1} \mathbf{a}_0 \tag{5}$$

MPDR can form beam gains in the LOS signal direction to increase the C/N$_0$, hence it can reduce the DLL variance. In the case where multipath falls into the side lobe of the beam, it also reduces the bias by decreasing the amplitude ratio α.

2.3. LCMP (multipath DOA required). The development of smart cities provides a chance to obtain the multipath DOA by 3D city model and ray tracing technique (Hsu et al. 2016), which is the motivation to nullify multipath in the pre-correlation structure. The beam null forming method LCMP is used in this paper to assist our discussion. The objective function of LCMP is given by (Wu et al. 2018; Jia et al. 2018)

$$\begin{cases} \min \ \mathbf{w}_{\mathrm{LCMP}}^{\mathrm{H}} \mathbf{R} \mathbf{w}_{\mathrm{LCMP}} \\ \text{s.t.} \ \ \mathbf{w}_{\mathrm{LCMP}}^{\mathrm{H}} \mathbf{C} = \mathbf{f} \end{cases} \tag{6}$$

where $\mathbf{C} = \begin{bmatrix} \mathbf{a}_0 & \hat{\mathbf{a}}_1 \end{bmatrix}$ is the beam constraint matrix, $\mathbf{f} = \begin{bmatrix} 1 & 0 \end{bmatrix}^{\mathrm{T}}$. The steer vector is denoted as $\hat{\mathbf{a}}_1 = \mathbf{a}\left(\hat{\theta}_1, \varphi_0\right)$, where multipath azimuth $\hat{\theta}_1$ can be obtained by 3D city model and ray tracing (Hsu et al. 2016). The solution to (6) is

$$\mathbf{w}_{\mathrm{LCMP}} = \mathbf{R}^{-1} \mathbf{C} \left(\mathbf{C}^{\mathrm{H}} \mathbf{R}^{-1} \mathbf{C} \right)^{-1} \mathbf{f} \tag{7}$$

The multiple constraints of LCMP is not only for passing the LOS signal without distortion, but also for forming beam null in the multipath direction. Therefore, LCMP gains more benefits in DLL bias reduction.

3. PROPOSED BEAM FORMING STRUCTURE. As it is mentioned in the previous section that beam forming has the superiority in improving GNSS performance in urban area for satellite signal enhancement and multipath mitigation. However, the required information, e.g., DOA of multipath, for multipath mitigation can only be obtained after correlation, the state-of-the-art beam forming methods to nullify multipath are implemented in the post-correlation structure (shown in Figure 1(d)). The post-correlation beam forming requires major change of the off-the-shelf GNSS receiver, and high computation load. In this section, the equivalent quiescent beam forming, which can be implemented as the pre-correlation structure as shown in Figure 1(c), is proposed to improve GNSS performance in urban area.

3.1. Quiescent beam forming.

Since the noise and signals are independent to each other, the covariance matrix can be reorganized as

$$\begin{aligned} \mathbf{R} &= \mathrm{E}\left[\left(\mathbf{x}_{\mathrm{s}} + \mathbf{x}_{\mathrm{m}} + \mathbf{x}_{\mathrm{n}} \right) \left(\mathbf{x}_{\mathrm{s}} + \mathbf{x}_{\mathrm{m}} + \mathbf{x}_{\mathrm{n}} \right)^{\mathrm{H}} \right] \\ &= \mathrm{E}\left[\left(\mathbf{x}_{\mathrm{s}} + \mathbf{x}_{\mathrm{m}} \right) \left(\mathbf{x}_{\mathrm{s}} + \mathbf{x}_{\mathrm{m}} \right)^{\mathrm{H}} \right] + \mathrm{E}\left[\mathbf{x}_{\mathrm{n}} \mathbf{x}_{\mathrm{n}}^{\mathrm{H}} \right] \end{aligned} \tag{8}$$

The SNR of the received LOS satellite signals before correlation is about -20dB (Wu et al. 2018).The SNR of the reflected signal is even lower due to the reflection loss. Therefore, the first part in (8) can be neglected, then the covariance matrix can be approximated by

$$\mathbf{R} \approx \mathrm{E}\left[\mathbf{x}_{\mathrm{n}} \mathbf{x}_{\mathrm{n}}^{\mathrm{H}} \right] = \sigma_{\mathrm{n}}^2 \mathbf{I} \tag{9}$$

Inserting (9) into the beam forming weights in (5) and (7), we can get

$$\mathbf{w}_{\mathrm{MPDR}} = \mathbf{a}_0 / \left\| \mathbf{a}_0 \right\|^2 = \mathbf{a}_0 / L = \mathbf{w}_{\mathrm{DRQ}} \tag{10}$$

and

$$\mathbf{w}_{\mathrm{LCMP}} = \mathbf{C} \left(\mathbf{C}^{\mathrm{H}} \mathbf{C} \right)^{-1} \mathbf{f} = \mathbf{w}_{\mathrm{LCQ}} \tag{11}$$

It is noted that (10) and (11) are independent with the received data $\mathbf{x}(t)$, the new ones are termed as quiescent beam forming weights (van Veen 1990). To differentiate from the original data dependent adaptive beam forming weights $\mathbf{w}_{\mathrm{MPDR}}$ and $\mathbf{w}_{\mathrm{LCMP}}$, the new terms $\mathbf{w}_{\mathrm{DRQ}}$ and $\mathbf{w}_{\mathrm{LCQ}}$ are defined as the Distortionless Response Quiescent (DRQ) and Linear Constraint Quiescent (LCQ) beam forming weights respectively.

The above derivation reveals that the pre-correlation adaptive beam forming in GNSS applications is equivalent to the quiescent beam forming. There is no need to calculate the covariance matrix and its inversion in quiescent beam forming, which greatly helps in decreasing the computational load and avoiding the problems of signal cancellation and correlation matrix rank deficiency.

The flow chart of the proposed pre-correlation receiver structure is given in Figure 2, where the solid line and boxes are for both the DRQ and LCQ processing, the dash line and boxes is for LCQ beam forming only. DOA of the LOS signal for beam gain forming required in (10) and (11) can be obtained by the satellite ephemeris and the coarse receiver position. The required multipath DOA in (11) for beam null forming can be promised by the 3D city model and ray-tracing. It is noted that both the DOAs of the LOS satellite signals and the multipath are independent of the received data and the array antenna, therefore, the obtained beam forming weight quality is independent to the antenna array aperture. The beam forming is applied to each of the satellite signals to enhance the LOS signal power, the multiple input from antenna array after beam forming become single output which is then sent to the tracking module.
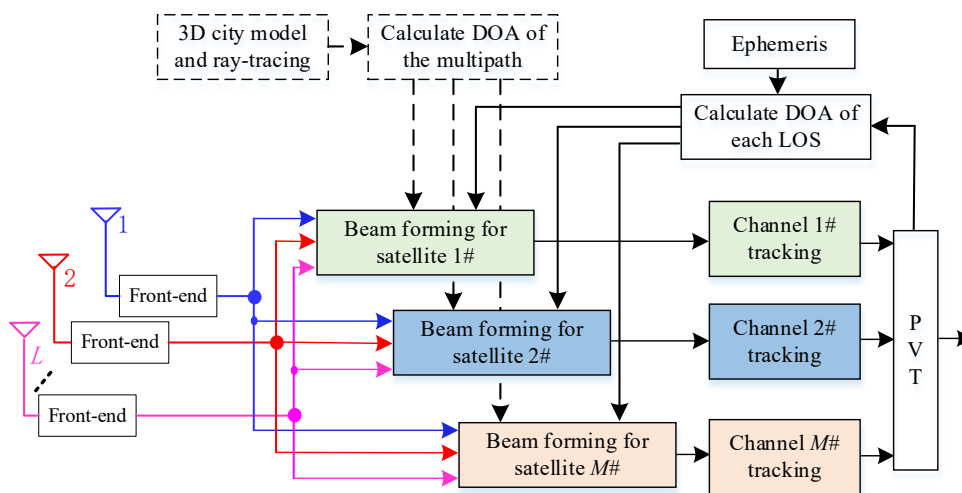

Figure 2 – Flow chart of the proposed receiver structure

3.2. Computational Complexities. The state-of-the-art beam forming structure for GNSS multipath mitigation is implemented as a post-correlation structure, which requires a major change of the off-the-shelf receiver structure. A number of extra tracking channels are required since signals from each array element need to be processed. The proposed structure in Figure 2 doesn't require extra tracking resources, hence it greatly reduces the system complexity. In addition, calculation of the covariance matrix (with a computation complexity of $O(L^2)$) and its inversion (with a computation complexity of $O(L^3)$) are avoided in the quiescent beam forming weights. Therefore, the proposed beam forming for GNSS multipath mitigation has low computation complexity.

4. PERFORMANCE ASSESSMENT MODEL. GNSS positioning performance is determined by the pseudorange quality and the dilution of precision of in-view satellites. Therefore, pseudorange quality is a key metric to describe the positioning performance. Since code phase obtained from the Delay Lock Loop (DLL) is commonly used to calculate the pseudorange, DLL performance is given below to illustrate the pseudorange quality. It should be pointed out that the coherent code discriminator is taken as an example in this paper, and the obtained results can be extended to non-coherent discriminator directly.

4.1. Variance from noise. It is revealed that the C/N0 is related with the variance of a coherent DLL by (Betz and Kolodziejski 2009a)

$$\sigma^2_{\text{DLL}} = \frac{B_L \int_{-B/2}^{B/2} G(f)\sin^2\left(\pi f d_{space}\right) df}{(2\pi)^2 \, \text{C/N}_0 \left(\int_{-B/2}^{B/2} fG(f)\sin\left(\pi f d_{space}\right) df\right)^2} \tag{12}$$

where B_L denotes the bandwidth of DLL, $G(f)$ is the normalized power spectra density of the satellite signal over the front-end bandwidth B. Equation (12) defines the variance of code phase estimation in white noise background. It is noted from (12) that DLL variance is inversely proportional to C/N0, as also shown in Figure 3(a), hence increasing C/N0 has a great potential to decrease the variance of DLL. The Signal-to-Noise Ratio (SNR) in Figure 3(a) is related with C/N0 by $\text{C/N}_0 = \text{SNR} \cdot B$.
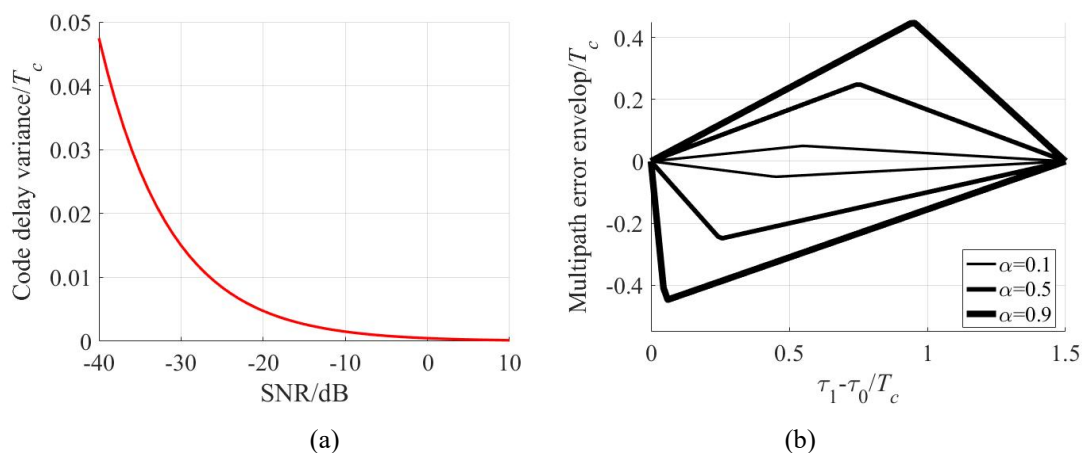

Figure 3 - Performance metrics: (a) variance, (b) bias.

It should be pointed out that (12) is the variance of a coherent DLL discriminator, the variance for a non-coherent DLL discriminator can be found in (Betz and Kolodziejski 2009b).

As proved in the appendix, the DLL variance after DRQ beam forming is

$$\sigma^2_{\text{DLL,DRQ}} = \frac{B_L \int_{-B/2}^{B/2} G(f)\sin^2\left(\pi f d_{space}\right) df}{(2\pi)^2 \left(\dfrac{L\iota_0^2}{\sigma^2} B\right)\left(\int_{-B/2}^{B/2} fG(f)\sin\left(\pi f d_{space}\right) df\right)^2} \tag{13}$$

After LCQ beam forming, the DLL variance is

$$\sigma^2_{\text{DLL,LCQ}} = \frac{B_L \int_{-B/2}^{B/2} G(f)\sin^2\left(\pi f d_{space}\right) df}{(2\pi)^2 \left(\dfrac{\iota_0^2\left(L^2 - \mu^2\right)}{L\sigma^2} B\right)\left(\int_{-B/2}^{B/2} fG(f)\sin\left(\pi f d_{space}\right) df\right)^2} \tag{14}$$

where μ is defined in the appendix as the correlation between LOS signal's and the reflected multipath's steering vector.

4.2. Bias from multipath. It is known that DLL bias caused by multipath can be evaluated by the MultiPath Error Envelope (MPEE) below (Liu and Amin 2009; Luo et al. 2016)

$$\varepsilon \approx \frac{\pm\alpha\int_{-B/2}^{B/2}G(f)\sin\left(\pi fd_{space}\right)\sin\left(2\pi f\Delta\tau\right)df}{2\pi\int_{-B/2}^{B/2}fG(f)\sin\left(\pi fd_{space}\right)\left[1\pm\alpha\cos\left(2\pi f\Delta\tau\right)\right]df} \tag{15}$$

where d_{space} is the spacing between the early and the late correlators, $\Delta\tau = \tau_1 - \tau_0$ is the relative code phase between the multipath and the LOS signal, and $\alpha = \iota_1/\iota_0$ is their amplitude ratio. The symbols '+' and '-' stand for two extreme cases of positive and negative maximum errors when the reflected signal is in-phase ($\Delta\phi = \phi_1 - \phi_0 = 0°$) or out-of-phase ($\Delta\phi = \pm180°$) with the LOS signal, respectively. The MPEE for different values of α with infinite bandwidth is shown in Figure 3(b), where T_c is the code width. It is shown in Figure 3(b) that the maximal value of MPEE is proportional to the amplitude ratio α. Multipath mitigation is to decrease the contribution of multipath in the contaminated data, hence it will compress MPEE to the *x* axis. To narrate the overall performance including all possible $\Delta\tau$, the Average MultiPath Error Envelop (AMPEE) is defined as (Markus et al. 2005)

$$S = \int_0^{\Delta\tau_{max}}\varepsilon d\left(\Delta\tau\right) \tag{16}$$

It is clearly noted from this section that the GNSS positioning performance in urban area is restricted by the low C/N$_0$ induced pseudorange variance and multipath induced pseudorange bias.

The MPEE after DRQ beam forming is

$$\varepsilon_{DRQ} = \frac{\pm\sqrt{\frac{\xi^2\iota_1^2}{\iota_0^2}}\int_{-B/2}^{B/2}G(f)\sin\left(\pi fd_{space}\right)\sin\left(2\pi f\Delta\tau\right)df}{2\pi\int_{-B/2}^{B/2}fG(f)\sin\left(\pi fd_{space}\right)\left[1\pm\sqrt{\frac{\xi^2\iota_1^2}{\iota_0^2}}\cos\left(2\pi f\Delta\tau\right)\right]df} \tag{17}$$

and the MPEE after LCQ beam forming is

$$\varepsilon_{LCQ} = \frac{\pm\sqrt{\frac{\left[\gamma\left(L\eta - \beta\mu\right)\iota_1\right]^2}{\iota_0^2}}\int_{-B/2}^{B/2}G(f)\sin\left(\pi fd_{space}\right)\sin\left(2\pi f\Delta\tau\right)df}{2\pi\int_{-B/2}^{B/2}fG(f)\sin\left(\pi fd_{space}\right)\left[1\pm\sqrt{\frac{\left[\gamma\left(L\eta - \beta\mu\right)\iota_1\right]^2}{\iota_0^2}}\cos\left(2\pi f\Delta\tau\right)\right]df} \tag{18}$$

where the detail of the defined variables ξ β, η, γ can be find in the appendix.

Equations (13)-(14) can be used to evaluate the DLL variance after beam forming, the variance reduction can be obtained by comparing to the ones before beam forming, which is the beam forming introduced profits. Similarly, (17)-(18) can be used to evaluate the DLL bias after beam forming, the bias reduction can be obtained by comparing to the ones before beam forming, which is another beam forming introduced profits. The derived assessment models can be used by the industry to calculate beam forming introduced performance improvement in terms of GNSS measurement. Therefore, they can balance among the

required performance, the cost budget and the available room for antenna placement straight-forwardly.

5. NUMERICAL SIMULATIONS AND PERFORMANCE ASSESSMENT RESULTS. Numerical results are given in this section. Firstly, by setting specific LOS and multipath parameters, e.g. DOAs, code phases, etc., the beam forming results are given. Secondly, the proposed model are validated by Monte Carlo simulations. Thirdly, the beam forming performance for all possible signal parameters are given ın a probability manner to assess the overall profits. Throughout the experiments, the GPS L1 signal is taken as an example, and the sampling frequency is 5.714 MHz, the receiver bandwidth is 4 MHz, the bandwidth of DLL loop filter is 2 Hz, and the DLL correlator spacing $d_{space} = T_c$. In addition, only one reflected multipath combined with the LOS signal is considered firstly, and multiple multipath will be discussed later.

5.1. Beam forming gain. The numerical results shown in Figure 4 present a qualitative assessment of the pre-correlation beam forming structure regarding DLL performance. The array antenna is a 3 by 3 rectangle array with a commonly used 0.5λ element spacing. The LOS signal incident into the array antenna has an SNR of -20dB, and $(\theta_0, \varphi_0)=(0°,30°)$ The DOA of multipath is $(\theta_1, \varphi_0)=(150°,30°)$. The amplitude ratio is $\alpha = \iota_1/\iota_0 = 0.5$, and the relative code phase is $\Delta\tau = \tau_2 - \tau_1 = 0.1T_c$. Figure 4(a) and (b) are the beam patterns of DRQ and LCQ, respectively.
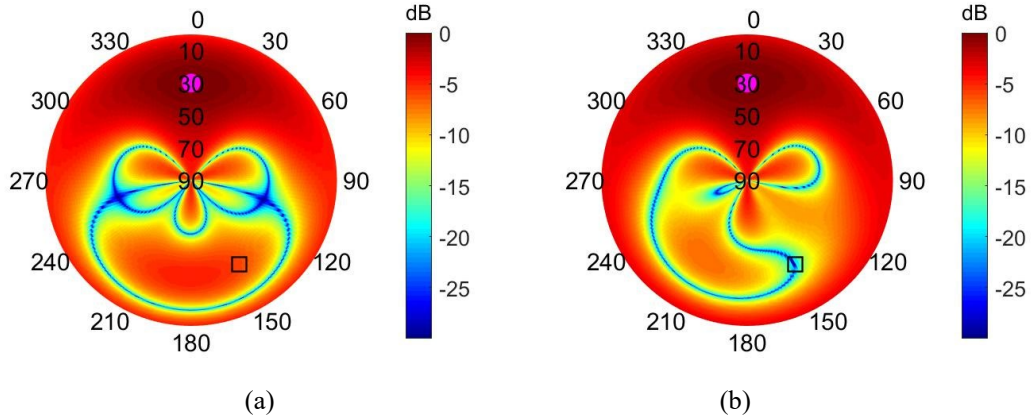

Figure 4 - Beam pattern: (a) DRQ, (b) LCQ

The DRQ forms beam gain in the LOS direction showing its ability to DLL variance reduction. The multipath bias can be reduced when the multipath falls into the beam side lobe. LCQ also forms beam null in multipath direction, hence it has much stronger ability to reduce multipath bias. However, in case of the multipath DOA close to the LOS, the beam distortion will cause signal loss.

Figure 5 compares the signal quality before and after beam forming, where Figure 5(a) compares the correlation functions of the received data from reference array element and data after the two beam forming patterns mentioned above. Figure 5(b) compares the MPEE in terms of the relative code phase $\Delta\tau = 0 \sim 1.5T_c$. It can be seen from Figure 5(a) that, although the correlation function is nearly submerged into noise for destructive multipath in the received data, the two curves after beam forming is close to the ideal one. For MPEE, the beam forming-based multipath mitigation is not restricted by the relative code phase, hence it has big advantages for short-delay multipath mitigation. Besides, since LCQ form beam null in

multipath direction, it performs better in multipath bias reduction. Multipath is only attenuated by the side lobe of DRQ, hence bias reduction by DRQ is limited by the side lobe power.
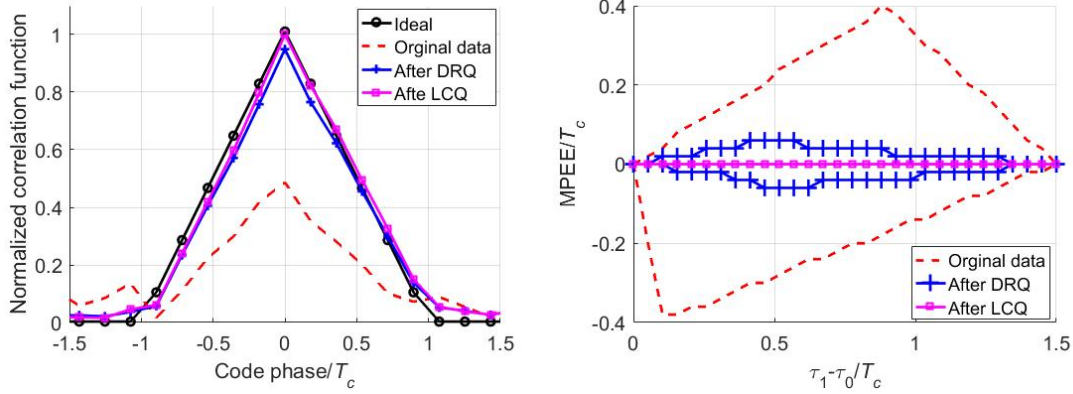

Figure 5 - Performance comparison: (a) correlation function, (b) MPEE

TABLE 2
DLL VARIANCE REDUCTION

Input setting	SNR (dB)	-40	-30	-20
Array setting	C/N_0 (dB-Hz)	26	36	46
	$\sigma_{before-BF}$ (m)	20.3	6.4	2.0
2 by 2	$\text{Min}\left(\sigma_{after-BF}\right)$ (m)	10.2	3.2	1
	$\text{Max}\left(\sigma_{after-BF} - \sigma_{before-BF}\right)$ (m)	10.2	3.2	1
3 by 3	$\text{Min}\left(\sigma_{after-BF}\right)$ (m)	6.8	2.1	0.6
	$\text{Max}\left(\sigma_{after-BF} - \sigma_{before-BF}\right)$ (m)	13.5	4.3	1.4
4 by 4	$\text{Min}\left(\sigma_{after-BF}\right)$ (m)	5.1	1.6	0.5
	$\text{Max}\left(\sigma_{after-BF} - \sigma_{before-BF}\right)$ (m)	15.2	4.8	1.5

DLL variance reduction using the beam forming methods with different array settings (rectangle array antenna with element number given in the leftmost column) and for different input SNR are compared in Table 2, where $\sigma_{before-BF}$ stands for the DLL standard deviation for the received GNSS data. The variance reduction is different for DRQ and LCQ, hence the minimum $\text{Min}\left(\sigma_{after-BF}\right)$ and maximum $\text{Max}\left(\sigma_{after-BF} - \sigma_{before-BF}\right)$ standard deviation after beam forming are given. The result in Table 2 shows great advantage of beam forming in GNSS performance improvement, especially for low SNR scenarios.

5.2. Validation of the proposed model. Monte Carlo simulations results are given to verify the effectiveness of the proposed model. The array setting in this subsection is the same as in the previous subsection. The amplitude ratio is also $\alpha = \iota_1/\iota_0 = 0.5$. The elevation angle of the LOS signal and the multipath are all $30°$, the azimuth of the LOS signal is fixed at $0°$, while the azimuth of the multipath at $20°$, $70°$ and $270°$ are all tested to obtain results for different scenarios.

Figure 6 compares the MPEE before and after different beam forming methods, the results from the proposed model are denoted with (M), while the results from simulations are denoted

with (S). The results for different multipath scenarios are given in Figure 6(a), (b) and (c) respectively. As in (A.21), the Direct-to-Multipath Ratio (DMR) after LCQ is infinite theoretically, which results in the numerical results from the proposed model in (18) is NaN, therefore the curve "LCQ(M)" is not given in Figure 6. Actually, the infinite DMR after LCQ means that the multipath is completely mitigated, hence the multipath induced bias is then diminished, and the MPEE should be zero for all relative code delay. It is noted from Figure 6(a) that, after DRQ beam forming, the MPEE only decreases a bit, for the multipath is close to the LOS signal, and then the multipath falls into the main beam of DRQ. As the azimuth of multipath depart far from the LOS signal, as shown in Figure 6(b) and (c), the MPEE after DRQ is decreased to a larger extent. Besides, it is clearly noted from the results in Figure 6 that the results from the proposed model and the simulated ones are close to each other, therefore, the effectiveness of the proposed model in (17) and (18) is validated.
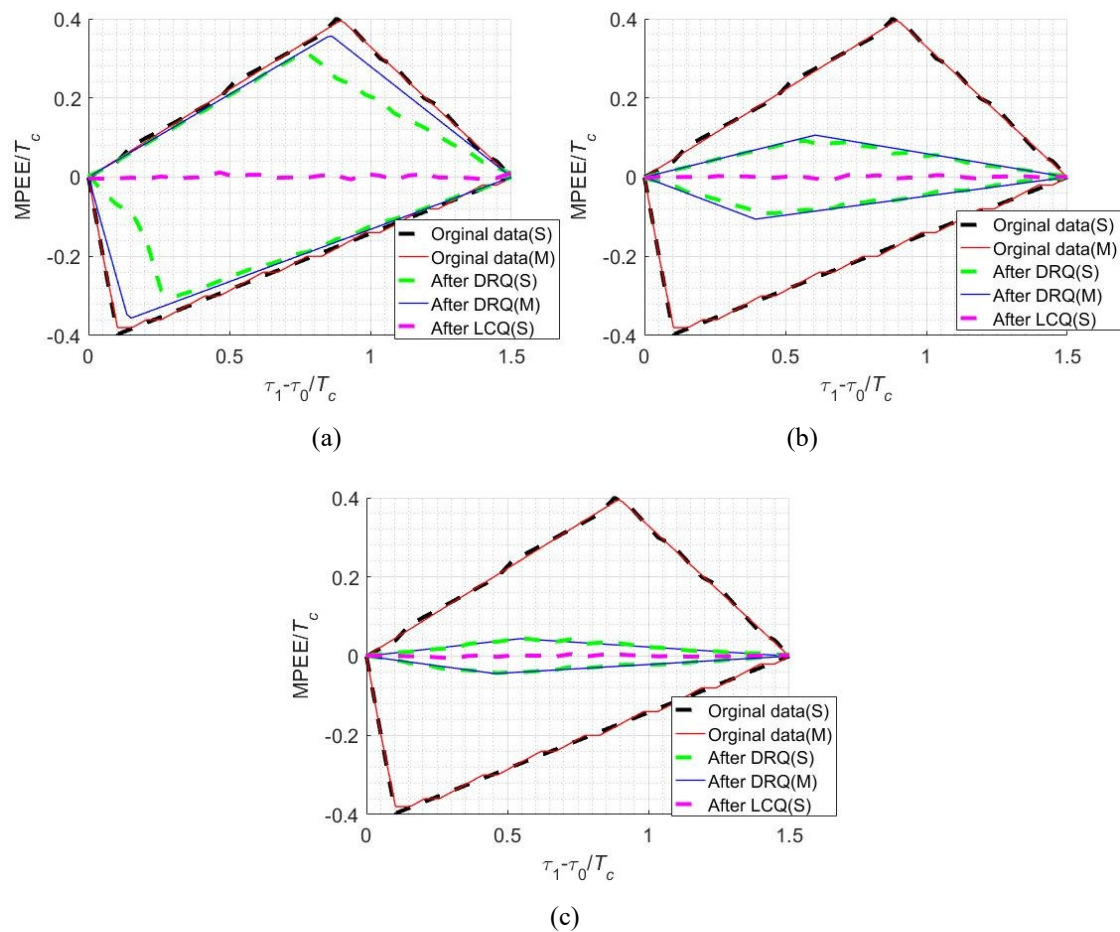

(a)

(b)

(c)

Figure 6 – MPEE from the proposed model and simulated ones for different multipath azimuth: (a) $\theta_1=20^0$, (b) $\theta_1=70^0$, (c) $\theta_1=270^0$

Figure 7 compares the code delay deviation reduction after different beam forming methods, the results from the proposed model are denoted with (M), while the results from simulations are denoted with (S). The results for different multipath scenarios are given in Figure 7(a), (b) and (c) respectively. It is clearly shown in Figure 7 that the simulated results and the results from the proposed model are almost overlapped together, therefore the effectiveness of the proposed model in (13) and (14) validated. It is noted from Figure 7(a) that, the code delay reduction after LCQ is smaller than the ones after DRQ. For when the multipath and the LOS signal are close to each other, the main beam of LCQ distorts, therefore the beam gain of LCQ is smaller than DRQ. As the azimuth of multipath depart

far from the LOS signal, the results shown in Figure 6(b) and (c), the code delay deviation reduction of DRQ and LCQ are almost the same.
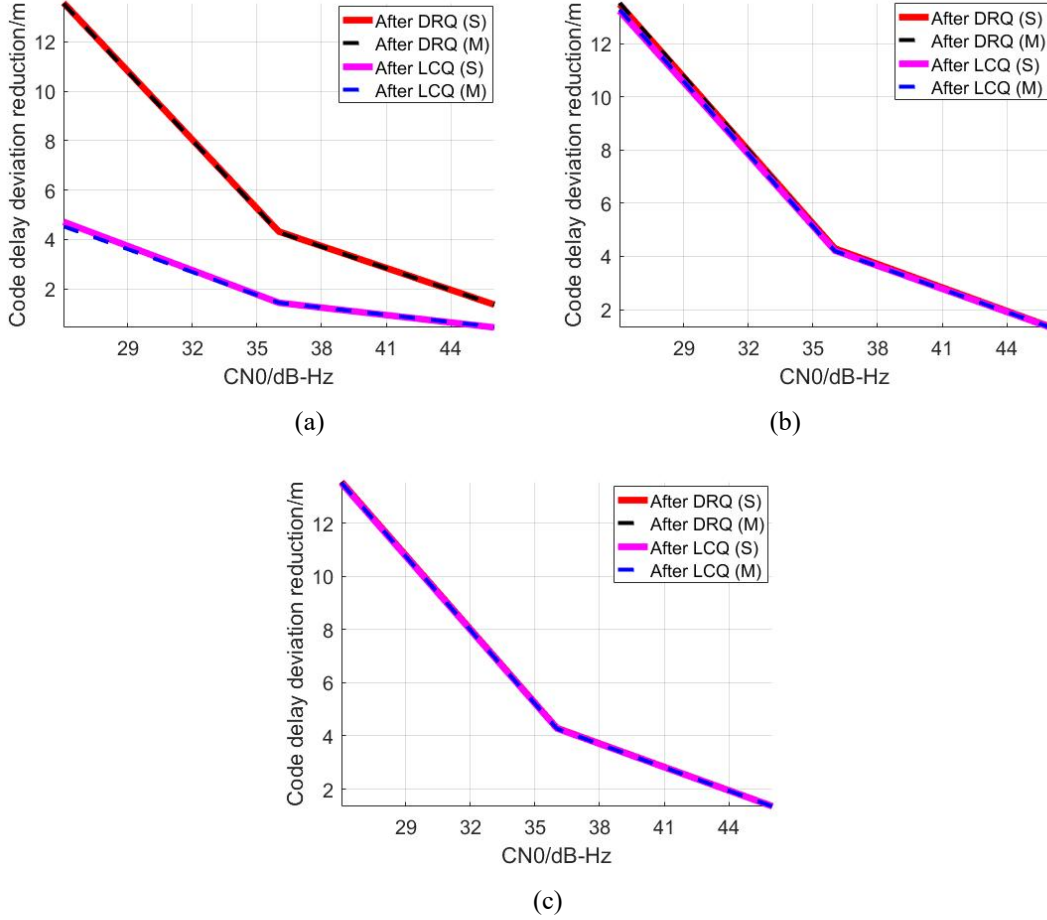

(a)

(b)

(c)

Figure 7 – Code delay deviation reduction from the proposed model and simulated ones for different multipath azimuth: (a) $\theta_1=20^0$, (b) $\theta_1=70^0$, (c) $\theta_1=270^0$

5.3. Different numbers of array element. To evaluate the overall performance, in this subsection we fix the LOS azimuth as $\theta_0=0°$ while changing the elevation angle and multipath azimuth in the whole spatial domain. For each multipath DOA, the corresponding DLL standard deviation reduction $\Delta\sigma = \sigma_{after-BF} - \sigma_{before-BF}$, and the AMPEE ratio $S_{after-BF}/S_{before-BF}$ are calculated.

Given SNR=-40dB (the corresponding C/N₀ is 26dB-Hz), Figure 8(a) shows the Cumulative Distribution Function (CDF) of variance reduction, and the CDF of bias reduction ratio is shown in Figure 8(b). The x-axis in Figure 8(a) is $\Delta\sigma$. It is noted that, DRQ has the full ability for DLL variance reduction, which can also be seen from **(A.**7) where the beam forming output SNR is proportional to the array element number and the input SNR. Hence the beam forming output SNR from DRQ will not change with the multipath DOA. When the DOA between the multipath and LOS signal is less than the beam width, the LCQ formed beam will be distorted, hence, it shows performance loss. Besides, the more array element number the narrower beam width, i.e., less distortion probability, which is also clearly shown in Figure 8. As the element number increases, the CDF of code phase variance reduction approaches to its steady-state much faster with a higher probability.

The DLL bias reduction using the two beam forming methods is almost an opposite situation as compared to variance reduction. By forming beam null, LCQ almost gets full performance in DLL bias reduction. In the extrema case that the LOS and multipath come from the same direction, the LCQ beam weight will be singular. For all other cases including the one where two DOAs difference is less than the beam width, the beam gain to the beam null ratio will be big enough to decrease the DLL bias, hence the bias reduction is almost 100%.

For DRQ, the bias reduction is much bigger when the multipath falls into the side lobe of the formed beam. When the DOA of multipath approaches to the LOS, the bias reduction performance degrades. When the two DOAs are equal to each other, there will be no bias reduction. Since more array element number means narrower beam width, the multipath has a higher probability to fall into the side lobe of the formed beam.
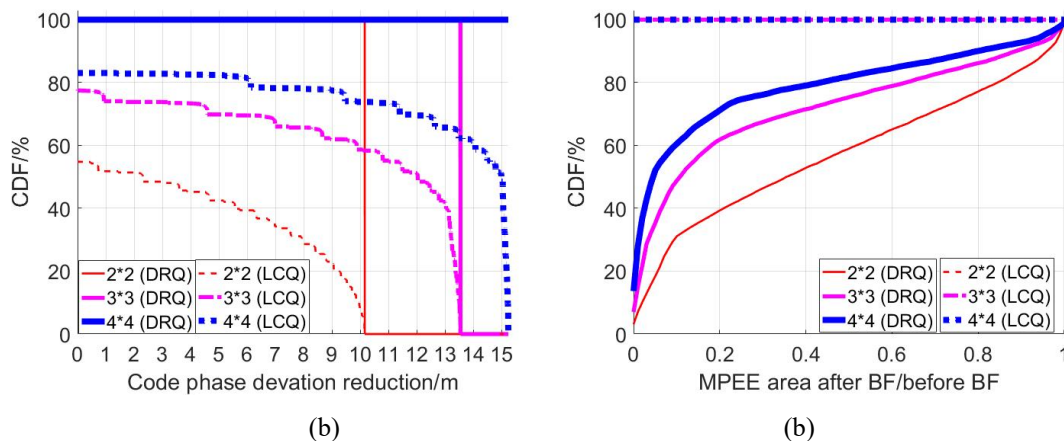

(b) (b)

Figure 8 - DLL performance improvement with different array element number: (a) variance reduction, (b) bias reduction

It can be concluded that, DRQ performs well in variance reduction, whereas LCQ is more useful for bias reduction. Noting that only the single multipath case is considered before. DRQ only form beam gain in the LOS direction, all the multipath incoming into the side lobe will be attenuated, hence it works for multiple multipath. LCQ form beam nulls in the multipath direction, the number of formed beam nulls is restricted by array element number. Therefore, LCQ for multiple multipath nulling requires more array elements.

5.4. Low cost setting of a 2 by 2 array. For low-cost applications, it is preferred to use less array elements and with only limited room for the antenna placement, hence we evaluate the DLL performance improvement of a 2 by 2 array by decreasing the element spacing from the commonly used 0.5λ to 0.25λ. The numerical results are given in Figure 9, where Figure 9(a) is the variance reduction and Figure 9(b) is the bias reduction.

As shown in Figure 9(a), the code variance reduction of DRQ is not affected by the element spacing. It is also the case in bias reduction of LCQ. Decreasing the element spacing to 0.4λ, LCQ in code variance reduction endures minor performance reduction. Further decreasing the element spacing, the performance loss will become much bigger, especially with the element spacing decreased to 0.3λ. The DRQ for bias reduction performance is also similar, hence it is better to keep the element spacing not less than 0.4λ (equals to 76mm for GPS L1). Figure 10 shows a smart phone, which is enough for a 2 by 2 rectangle antenna array, and much bigger room is available for vehicles. Therefore, widespread application of array antenna can be expected for urban positioning in future industry.
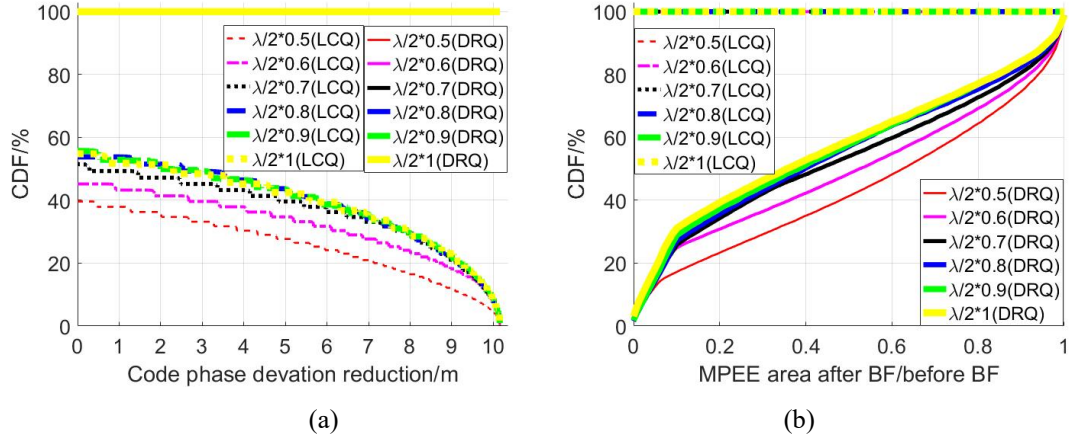
Figure 9 - DLL performance improvement with different element space: (a) variance reduction, (b) bias reduction
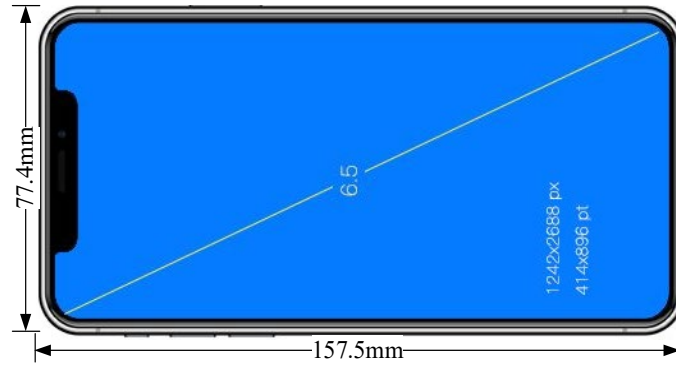

Figure 10 - Size of a smart phone

6. CONCLUSIONS AND SUGGESTIONS. A pre-correlation beam forming structure is suggested to improve GNSS performance for low cost urban positioning. It is not only compatible with the off-the-shelf receiver, but also decreases the computational load by using the equivalent quiescent beam forming weight. Based on the pre-correlation structure, theoretical models are established to assess the beam forming introduced performance improvement in terms of pesudorange quality. The model can serve as a tool for the industry to balance the minimum required performance, cost budget, and available room for antenna placement. The numerical results show that, a 2 by 2 rectangle array by using the DRQ quiescent beam forming weight is a good choice for cost-effective applications. The superiority of the suggested choice can be listed as: ① it does not require the multipath DOA information. ② it can provide 100% code phase deviation reduction in all possible LOS directions. ③ it can also provide 20% bias reduction with a probability nearly to 80%. Besides, the array element space can be reduced to about 0.4λ for only minor performance loss.

APPENDIX. DERIVATION OF THE ASSESSMENT MODEL. The beam forming profits to DLL performance is studied in this section. Applying the beam forming weight to the LOS satellite signal in the received data, we can get

$$
\begin{aligned}
y_{s,DRQ}(t) &= \mathbf{w}_{DRQ}^{H}\mathbf{x}_{s}(t) \\
&= \mathbf{a}_0^{H}\mathbf{a}_0 / L \iota_0 s_0(t) \\
&= \iota_0 s_0(t)
\end{aligned}
\tag{A.1}
$$

In fact, this is the constraint in (4) for passing the LOS signal without distortion. Similarly, the multipath is

$$
\begin{aligned}
y_{\mathrm{m,DRQ}}(t) &= \mathbf{w}_{\mathrm{DRQ}}^{\mathrm{H}} \mathbf{x}_{\mathrm{m}}(t) \\
&= \mathbf{a}_0^{\mathrm{H}} \mathbf{a}_1 / L \, \iota_1 s_1(t) \\
&= \xi \iota_1 s_1(t)
\end{aligned}
\tag{A.2}
$$

where

$$
\xi = \mathbf{a}_0^{\mathrm{H}} \mathbf{a}_1 / L \le 1
\tag{A.3}
$$

is the correlation coefficient of the LOS and multipath steer vectors. Further, the output power of the LOS signal is

$$
P_{\mathrm{s,DRQ}} = \mathrm{E}\left[\left| y_{\mathrm{s}}(t) \right|^2\right] = \iota_0^2
\tag{A.4}
$$

The power of multipath is

$$
P_{\mathrm{m,DRQ}} = \mathrm{E}\left[\left| y_{\mathrm{m}}(t) \right|^2\right] = \xi^2 \iota_1^2
\tag{A.5}
$$

And the noise power is

$$
\begin{aligned}
P_{\mathrm{n,DRQ}} &= \mathrm{E}\left[\left| \mathbf{w}_{\mathrm{DRQ}}^{\mathrm{H}} \mathbf{x}_{\mathrm{n}}(t) \right|^2\right] \\
&= \mathbf{w}_{\mathrm{DRQ}}^{\mathrm{H}} \mathrm{E}\left[\mathbf{x}_{\mathrm{n}}(t) \mathbf{x}_{\mathrm{n}}^{\mathrm{H}}(t) \right] \mathbf{w}_{\mathrm{DRQ}} \\
&= \sigma^2 \mathbf{w}_{\mathrm{DRQ}}^{\mathrm{H}} \mathbf{w}_{\mathrm{DRQ}} \\
&= \sigma^2 \mathbf{a}_0^{\mathrm{H}} \mathbf{a}_0 / L^2 = \sigma^2 / L
\end{aligned}
\tag{A.6}
$$

Hence the output SNR can be calculated as

$$
\mathrm{SNR}_{\mathrm{out,DRQ}} = P_{\mathrm{s,DRQ}} / P_{\mathrm{n,DRQ}} = L \iota_0^2 / \sigma^2
\tag{A.7}
$$

The power ratio of the LOS signal to the multipath, which we defined as Direct-to-Multipath Ratio (DMR) can be given as

$$
\mathrm{DMR}_{\mathrm{out,DRQ}} = P_{\mathrm{s,DRQ}} / P_{\mathrm{m,DRQ}} = \iota_0^2 / \xi^2 \iota_1^2
\tag{A.8}
$$

It is noted from (A.7) that the output SNR of DRQ is proportional to the array element number L. The output DMR in (A.8) is affected by DOA difference between the LOS and multipath.

To analyze the LCQ beam forming, expand equation (11) as

$$
\mathbf{w}_{\mathrm{LCQ}} = 1 / \left(L^2 - \mathbf{a}_0^{\mathrm{H}} \hat{\mathbf{a}}_1 \hat{\mathbf{a}}_1^{\mathrm{H}} \mathbf{a}_0 \right) \times \begin{bmatrix} \mathbf{a}_0 & \hat{\mathbf{a}}_1 \end{bmatrix} \begin{bmatrix} L & -\mathbf{a}_0^{\mathrm{H}} \hat{\mathbf{a}}_1 \\ -\hat{\mathbf{a}}_1^{\mathrm{H}} \mathbf{a}_0 & L \end{bmatrix} \begin{bmatrix} 1 \\ 0 \end{bmatrix}
\tag{A.9}
$$

Let

$$
\gamma = 1 / \left(L^2 - \mathbf{a}_0^{\mathrm{H}} \hat{\mathbf{a}}_1 \hat{\mathbf{a}}_1^{\mathrm{H}} \mathbf{a}_0 \right)
\tag{A.10}
$$

Equation (A.9) can then be simplified to

$$
\mathbf{w}_{\mathrm{LCQ}} = \gamma \left[L \mathbf{a}_0 - \hat{\mathbf{a}}_1 \hat{\mathbf{a}}_1^{\mathrm{H}} \mathbf{a}_0 \right]
\tag{A.11}
$$

Applying the above weight to the signal component, we can get

$$y_{s,LCQ}(t) = \mathbf{w}_{LCQ}^{H}\mathbf{x}_{s}(t)$$
$$= \gamma \left[L\mathbf{a}_0^{H} - \mathbf{a}_0^{H}\hat{\mathbf{a}}_1\hat{\mathbf{a}}_1^{H} \right]\mathbf{a}_0 \iota_0 s_0(t)$$
$$= \gamma \left[L\mathbf{a}_0^{H}\mathbf{a}_0 - \mathbf{a}_0^{H}\hat{\mathbf{a}}_1\hat{\mathbf{a}}_1^{H}\mathbf{a}_0 \right]\iota_0 s_0(t) \tag{A.12}$$
$$= \iota_0 s_0(t)$$

It should be pointed out that the above equations holds when $\theta_0 \neq \hat{\theta}_1$, in case the LOS and multipath come from the same direction, all spatial beam forming methods became invalid.

Similarly, the multipath component after beam forming is

$$y_{m,LCQ}(t) = \mathbf{w}_{LCQ}^{H}\mathbf{x}_{m}(t)$$
$$= \gamma \left[L\mathbf{a}_0^{H}\mathbf{a}_1 - \mathbf{a}_0^{H}\hat{\mathbf{a}}_1\hat{\mathbf{a}}_1^{H}\mathbf{a}_1 \right]\iota_1 s_1(t) \tag{A.13}$$

Let

$$\beta = \hat{\mathbf{a}}_1^{H}\mathbf{a}_1, \ \eta = \mathbf{a}_0^{H}\mathbf{a}_1, \mu = \mathbf{a}_0^{H}\hat{\mathbf{a}}_1 \tag{A.14}$$

Inserting (A.14) into (A.13), we can get

$$y_{m,LCQ}(t) = \gamma\left(L\eta - \beta\mu \right)\iota_1 s_1(t) \tag{A.15}$$

If there is no estimation error of the multipath DOA (i.e., $\hat{\mathbf{a}}_1 = \mathbf{a}_1$, $\beta = \hat{\mathbf{a}}_1^{H}\mathbf{a}_1 = L$), then we have $y_{m,LCQ}(t) = 0$, which is another constraint in (6) to nullify multipath. Since the reflection point is close to the receiver, the uncertainty of the receiver position will result in DOA error of the multipath, hence we have $\beta \leq L$. The correlation coefficient η in (A.14) stands for the similarity between the LOS and multipath steer vectors. Obviously, the formed beam gain and null will not be affected by each other as the two steer vectors are orthogonal. On the contrary, when the two components are close in the spatial domain, the beam will be distorted.

The output signal power after LCQ beam forming is

$$P_{s,LCQ} = E\left[\left| y_{s,LCQ}(t) \right|^2 \right] = \iota_0^2 \tag{A.16}$$

The residual multipath power is

$$P_{m,LCQ} = E\left[\left| y_{m,LCQ}(t) \right|^2 \right]$$
$$= \left[\gamma\left(L\eta - \beta\mu \right)\iota_1 \right]^2 \tag{A.17}$$

The noise power is

$$P_{n,LCQ} = \sigma^2 \mathbf{w}_{LCQ}^{H}\mathbf{w}_{LCQ} \tag{A.18}$$

The norm of the LCQ weight can be calculated as

$$\mathbf{w}_{LCQ}^{H}\mathbf{w}_{LCQ} = \left[\mathbf{C}\left(\mathbf{C}^{H}\mathbf{C} \right)^{-1}\mathbf{f} \right]^{H}\mathbf{C}\left(\mathbf{C}^{H}\mathbf{C} \right)^{-1}\mathbf{f}$$
$$= \mathbf{f}^{H}\left(\mathbf{C}^{H}\mathbf{C} \right)^{-1}\mathbf{f}$$
$$= L/\left(L^2 - \mathbf{a}_0^{H}\hat{\mathbf{a}}_1\hat{\mathbf{a}}_1^{H}\mathbf{a}_0 \right) \tag{A.19}$$
$$= L/\left(L^2 - \mu^2 \right)$$

Using (A.16), (A.18) and (A.19), the output SNR can be calculated as

$$\begin{aligned} \text{SNR}_{\text{out,LCQ}} &= P_{\text{s,LCQ}}/P_{\text{n,LCQ}} \\ &= \iota_0^2\left(L^2 - \mu^2\right)/L\sigma^2 \end{aligned}$$

(A.20)

Similarly, using (A.16) and (A.17), the DMR is

$$\begin{aligned} \text{DMR}_{\text{out,LCQ}} &= P_{\text{s,LCQ}}/P_{\text{m,LCQ}} \\ &= \iota_0^2\Big/\left[\gamma\left(L\eta - \beta\mu\right)\iota_1\right]^2 \end{aligned}$$

(A.21)

According to (A.7)-(A.8), and (A.20)-(A.21), the output SNR and DMR from beam forming is related to ξ for DRQ, and β, η, γ, for LCQ, respectively. As the definition of these variables show ((A.3), (A.10) and (A.14)), they are related with the array setting, e.g., element number, element spacing, multipath DOA, DOA difference between the LOS and multipath, etc.. Therefore, the beam forming profits can be evaluated by setting these parameters.

To depict the beam forming gain to the DLL performance, firstly we calculate the C/N_0 by the obtained SNR in (A.4) and (A.20) as

$$C/N_{0\,\text{out,DRQ}} = L\iota_0^2 B/\sigma^2$$

(A.22)

and

$$C/N_{0\,\text{out,LCQ}} = \iota_0^2\left(L^2 - \mu^2\right)B/L\sigma^2$$

(A.23)

By inserting (A.22) into (12), the DLL variance can be obtained

$$\sigma_{\text{DLL,DRQ}}^2 = \frac{B_L\int_{-B/2}^{B/2}G(f)\sin^2\left(\pi f d_{space}\right)\mathrm{d}f}{(2\pi)^2\left(\dfrac{L\iota_0^2}{\sigma^2}B\right)\left(\int_{-B/2}^{B/2}fG(f)\sin\left(\pi f d_{space}\right)\mathrm{d}f\right)^2}$$

(A.24)

For LCQ, inserting (A.23) into (12), we have

$$\sigma_{\text{DLL,LCQ}}^2 = \frac{B_L\int_{-B/2}^{B/2}G(f)\sin^2\left(\pi f d_{space}\right)\mathrm{d}f}{(2\pi)^2\left(\dfrac{\iota_0^2\left(L^2 - \mu^2\right)}{L\sigma^2}B\right)\left(\int_{-B/2}^{B/2}fG(f)\sin\left(\pi f d_{space}\right)\mathrm{d}f\right)^2}$$

(A.25)

Given the DMR in (A.8) and (A.21), the amplitude ratio α can be obtained, further inserting α into (15), the MPEE are obtained as

$$\varepsilon_{\text{DRQ}} = \frac{\pm\sqrt{\dfrac{\xi^2\iota_1^2}{\iota_0^2}}\int_{-B/2}^{B/2}G(f)\sin\left(\pi f d_{space}\right)\sin\left(2\pi f\Delta\tau\right)\mathrm{d}f}{2\pi\int_{-B/2}^{B/2}fG(f)\sin\left(\pi f d_{space}\right)\left[1\pm\sqrt{\dfrac{\xi^2\iota_1^2}{\iota_0^2}}\cos\left(2\pi f\Delta\tau\right)\right]\mathrm{d}f}$$

(A.26)

and

$$\varepsilon_{\text{LCQ}} = \frac{\pm\sqrt{\frac{\left[\gamma(L\eta - \beta\mu)\iota_1\right]^2}{\iota_0^2}} \int_{-B/2}^{B/2} G(f)\sin(\pi f d_{space})\sin(2\pi f \Delta\tau)\mathrm{d}f}{2\pi\int_{-B/2}^{B/2} fG(f)\sin(\pi f d_{space})\left[1 \pm \sqrt{\frac{\left[\gamma(L\eta - \beta\mu)\iota_1\right]^2}{\iota_0^2}}\cos(2\pi f \Delta\tau)\right]\mathrm{d}f} \tag{A.27}$$

REFERENCES

PUBLICATION BIBLIOGRAPHY

Alnaqbi A; El-Rabbany A (2010) Precise GPS Positioning with Low-Cost Single-Frequency System in Multipath Environment. In *J. Navigation* 63 (2), 301-312. DOI: 10.1017/S0373463309990373.

Amin MG; Closas P; Broumandan A et al. (2016) Vulnerabilities, threats, and authentication in satellite-based navigation systems [scanning the issue]. In *Proc. IEEE* 104 (6), 1169-1173. DOI: 10.1109/JPROC.2016.2550638.

Appel M; Iliopoulos A; Fohlmeister F et al. (2019) Interference and multipath suppression with space-time adaptive beamforming for safety-of-life maritime applications. In *CEAS Space J* 11 (1), 21-34. DOI: 10.1007/s12567-019-0236-x.

Aram M; El-Rabbany A; Krishnan S et al. (2007) Single Frequency Multipath Mitigation Based On Wavelet Analysis. In *J. Navigation* 60 (2), 281-290. DOI: 10.1017/S0373463307004146.

Betz JW; Kolodziejski KR (2009a) Generalized Theory of Code Tracking with an Early-Late Discriminator Part I: Lower Bound and Coherent Processing. In *IEEE Trans. Aerosp. Electron. Syst.* 45 (4), 1538-1556. DOI: 10.1109/TAES.2009.5310316.

Betz JW; Kolodziejski KR (2009b) Generalized Theory of Code Tracking with an Early-Late Discriminator Part II: Noncoherent Processing and Numerical Results. In *IEEE Trans. Aerosp. Electron. Syst.* 45 (4), 1557-1564. DOI: 10.1109/TAES.2009.5310317.

Broumandan A; Jafarnia-Jahromi A; Daneshmand S et al. (2016) Overview of Spatial Processing Approaches for GNSS Structural Interference Detection and Mitigation. In *Proc. IEEE* 104 (6), 1246-1257. DOI: 10.1109/JPROC.2016.2529600.

Bryan T; Patrick F (1995) Performance Evaluation of the Multipath Estimating Delay Lock Loop 42 (3), 502-514.

Bryan, Townsend; Patrick, Fenton (1994) A Practical Approach to the Reduction of Pseudorange Multipath Errors in a Ll GPS Receiver. *Proceedings of the 7th International Technical Meeting of the Satellite Division of The Institute of Navigation (ION GPS 1994)*. Salt Lake City, UT, September 20 - 23.

Caizzone Stefano; Elmarissi Wahid; Buchner Georg et al. (2016) Compact 6+1 antenna array for robust GNSS applications. *IEEE 2016 International Conference on Localization and GNSS (ICL-GNSS)*. Barcelona, Jun 28-30.

Cuntz M; Konovaltsev A; Meurer M (2016) Concepts, Development, and Validation of Multiantenna GNSS Receivers for Resilient Navigation. In *Proc. IEEE* 104 (6), 1288-1301. DOI: 10.1109/JPROC.2016.2525764.

Daneshmand S; Nielsen J; Broumandan A et al. (2013) Interference and multipath mitigation utilising a two-stage beamformer for global navigation satellite systems applications. In *IET Radar, Sonar & Navigation* 7 (1), 55-66. DOI: 10.1049/iet-rsn.2012.0027.

Fernandez-Prades C; Arribas J; Closas P (2016) Robust GNSS Receivers by Array Signal Processing: Theory and Implementation. In *Proc. IEEE* 104 (6), 1207-1220. DOI: 10.1109/JPROC.2016.2532963.

Fohlmeister F; Iliopoulos A; Sgammini M et al. (2017) Dual polarization beamforming algorithm for multipath mitigation in GNSS. In *Signal Processing* 138, 86-97. DOI: 10.1016/j.sigpro.2017.03.012.

Garca-Molina JA; Fernndez-Rubio JA; Parro JM (2018) Exploiting Spatial Diversity for NLOS Indoor Positioning. *31st International Technical Meeting of The Satellite Division of the Institute of Navigation (ION GNSS+ 2018).* Miami, Florida, 2018/9/24 - 2018/9/28: Institute of Navigation (ION GNSS+, The International Technical Meeting of the Satellite Division of The Institute of Navigation), 3457-3462.

García-Molina, J. A.; Fernández-Rubio, J. A. (2019) Array Processing and Unambiguous Positioning of Signals with Multi-Peak Correlations. *Proceedings of the 32nd International Technical Meeting of the Satellite Division of The Institute of Navigation (ION GNSS+ 2019).* Miami, Florida, September 16 - 20.

Gary, A. McGraw; Michael, S. Braasch (1999) GNSS Multipath Mitigation Using Gated and High Resolution Correlator Concepts. *Proceedings of the 1999 National Technical Meeting of The Institute of Navigation.* San Diego, CA, January 25 - 27.

Groves PD; Jiang Z (2013) Height Aiding, C / N0 Weighting and Consistency Checking for GNSS NLOS and Multipath Mitigation in Urban Areas. In *J. Navigation* 66 (5), 653-669. DOI: 10.1017/S0373463313000350.

Hsu, L-T. (2017) GNSS multipath detection using a machine learning approach. *2017 IEEE 20th International Conference on Intelligent Transportation Systems (ITSC).* Yokohama, Japan, Oct. 16-19. Piscataway, NJ: IEEE. Available online at http://ieeexplore.ieee.org/servlet/opac?punumber=8307147.

Hsu L-T (2018) Analysis and modeling GPS NLOS effect in highly urbanized area. In *GPS Solut* 22 (1), 59. DOI: 10.1007/s10291-017-0667-9.

Hsu L-T; Gu Y. Kamijo S (2016) 3D building model-based pedestrian positioning method using GPS/GLONASS/QZSS and its reliability calculation. In *GPS Solut* 20 (3), 413-428. DOI: 10.1007/s10291-015-0451-7.

Hsu L-T, Jan S-S, Groves PD et al. (2015) Multipath mitigation and NLOS detection using vector tracking in urban environments. In *GPS Solut* 19 (2), 249-262. DOI: 10.1007/s10291-014-0384-6.

J. A. Garcia-Molina; J. A. Fernandez-Rubio (2018) Positioning and Timing in the MIMO-GNSS Framework. *2018 9th ESA Workshop on Satellite NavigationTechnologies and European Workshop on GNSS Signals and Signal Processing (NAVITEC),* Dec. 5-7. Noordwijk, Netherlands.

Jia Q, Wu R, Wang W et al. (2017) Multipath interference mitigation in GNSS via WRELAX. In *GPS Solut* 21 (2), 487-498. DOI: 10.1007/s10291-016-0538-9.

Jia Q, Wu R, Wang W et al. (2018) Adaptive blind anti-jamming algorithm using acquisition information to reduce the carrier phase bias. In *GPS Solut* 22 (4), 13417. DOI: 10.1007/s10291-018-0764-4.

Li Q, Wang W, Xu D et al. (2014) A Robust Anti-Jamming Navigation Receiver with Antenna Array and GPS/SINS. In *IEEE Commun. Lett.* 18 (3), 467-470. DOI: 10.1109/LCOMM.2014.012314.132451.

Liu L; Amin MG (2009) Tracking performance and average error analysis of GPS discriminators in multipath. In *Signal Processing* 89 (6), 1224-1239. DOI: 10.1016/j.sigpro.2009.01.007.

Luo R, Xu Y. Yuan H (2016) Performance Evaluation of the New Compound-Carrier-Modulated Signal for Future Navigation Signals. In *Sensors (Basel, Switzerland)* 16 (2), 142. DOI: 10.3390/s16020142.

Markus, Berg; Rameez, U. Rahman LighariR; Jani, Kallankari et al. (2016) Polarization based measurement system for analysis of GNSS multipath signals. *2016 10th European Conference on Antennas and Propagation (EuCAP).* Davos, Switzerland, April 10-15.

Markus, Irsigler; Jose, Angel Avila-Rodriguez; Guenter, W. Hein (2005) Criteria for GNSS Multipath Performance Assessment. *Proceedings of the 18th International Technical Meeting of the Satellite Division of The Institute of Navigation (ION GNSS 2005).* Long Beach Convention Center, September 13 - 16.

Min Li, Andrew G. Dempster, Asghar T. Balaei et al. (2011) Switchable Beam Steering/Null Steering Algorithm for CW Interference Mitigation in GPS C/A Code Receivers. In *IEEE TRANSACTIONS ON AEROSPACE AND ELECTRONIC SYSTEMS* 47 (3), 1564-1579.

R.D.J. van Nee (1992a) Reducing multipath tracking errors in spread-spectrum ranging systems - Electronics Letters. In *Electronics Letters* 28 (8), 729-731.

R.D.J. van Nee (1992b) The Multipath Estimating Delay Lock Loop - Spread Spectrum Techniques and Applications. *IEEE Second International Symposium on Spread Spectrum Techniques and Applications,* Nov. 29- Dec. 2. Yokohama, Japan.

Realini E; Reguzzoni M (2013) goGPS: open source software for enhancing the accuracy of low-cost receivers by single-frequency relative kinematic positioning. In *Meas. Sci. Technol.* 24 (11), 115010. DOI: 10.1088/0957-0233/24/11/115010.

S. Daneshmand; A. Broumandan, N. Sokhandan et al. (2013) GNSS Multipath Mitigation with a Moving Antenna Array. IEEE Transactions on Aerospace and Electronic Systems 49 (1), 693-698.

Sahmoudi M; Amin MG (2009) Robust tracking of weak GPS signals in multipath and jamming environments. In *Signal Processing* 89 (7), 1320-1333. DOI: 10.1016/j.sigpro.2009.01.001.

Seco-Granados G; Fernandez-Rubio JA. Fernandez-Prades C (2005) ML estimator and hybrid beamformer for multipath and interference mitigation in GNSS receivers. In *IEEE Trans. Signal Process.* 53 (3), 1194-1208. DOI: 10.1109/TSP.2004.842193.

Sgammini M; Caizzone S; Hornbostel A et al. (2019) Interference mitigation using a dual‑polarized antenna array in a real environment. In *NAVIGATION* 66 (3), 523-535. DOI: 10.1002/navi.309.

Sokhandan N; Broumandan A; Curran JT et al. (2014) High Resolution GNSS Delay Estimation for Vehicular Navigation Utilizing a Doppler Combining Technique. In *J. Navigation* 67 (4), 579-602. DOI: 10.1017/S0373463313000830.

Sun R; Hsu L-T; Xue D et al. (2019) GPS Signal Reception Classification Using Adaptive Neuro-Fuzzy Inference System. In *J. Navigation* 72 (3), 685-701. DOI: 10.1017/S0373463318000899.

Sun R; Wang G; Zhang W et al. (2020) A gradient boosting decision tree based GPS signal reception classification algorithm. In *Applied Soft Computing* 86, 105942. DOI: 10.1016/j.asoc.2019.105942.

Tamazin M; Noureldin A; Korenberg MJ et al. (2016) A New High-Resolution GPS Multipath Mitigation Technique Using Fast Orthogonal Search. In *J. Navigation* 69 (4), 794-814. DOI: 10.1017/S0373463315001022.

Tranquilla JM; Carr JP. Al-Rizzo HM (1994) Analysis of a choke ring groundplane for multipath control in Global Positioning System (GPS) applications. In *IEEE Trans. Antennas Propagat.* 42 (7), 905-911. DOI: 10.1109/8.299591.

Vagle N; Broumandan A; Jafarnia-Jahromi A et al. (2016a) Performance analysis of GNSS multipath mitigation using antenna arrays. In *J. Glob. Position. Syst.* 14 (1), 265. DOI: 10.1186/s41445-016-0004-6.

Vagle N; Broumandan A; Lachapelle G (2016b) Analysis of Multi-Antenna GNSS Receiver Performance under Jamming Attacks. In *Sensors (Basel, Switzerland)* 16 (11). DOI: 10.3390/s16111937.

van Veen BD (1990) Optimization of quiescent response in partially adaptive beamformers. In *IEEE Trans. Acoust., Speech, Signal Processing* 38 (3), 471-477. DOI: 10.1109/29.106865.

Vicario, Jose Lopez; Barcelo, Marc; Manosas, Marti et al. (2010) A novel look into digital beamforming techniques for multipath and interference mitigation in Galileo Ground Stations. *Advanced satellite multimedia systems conference (asma) and the 11th signal processing for space communications workshop.*

Volakis JL; O'Brien AJ; Chen C-C (2016) Small and Adaptive Antennas and Arrays for GNSS Applications. In *Proc. IEEE* 104 (6), 1221-1232. DOI: 10.1109/JPROC.2016.2528165.

Wang Y; Huang Z (2019) MEDLL On-Strobe Correlator: A Combined Anti-multipath Technique for GNSS Signal Tracking. In *J. Navigation* 5, 1-20. DOI: 10.1017/S0373463319000870.

Wu R; Wang W; Lu D et al. (2018) Adaptive Interference Mitigation in GNSS. Singapore:: Springer Singapore.

Xie L; Cui X; Zhao S et al. (2017) Mitigating Multipath Bias Using a Dual-Polarization Antenna: Theoretical Performance, Algorithm Design, and Simulation. In *Sensors (Basel, Switzerland)* 17 (2). DOI: 10.3390/s17020359.

Xie P; Petovello MG (2015) Improved Correlator Peak Selection for GNSS Receivers in Urban Canyons. In *J. Navigation* 68 (5), 869-886. DOI: 10.1017/S037346331500017X.